

Synthesis, Microstructure, and Properties of High-Molar-Mass Polyglycolide Copolymers with Isolated Methyl Defects

Esra Altay,[†] Yoon-Jung Jang,[†] Xiang Qi Kua, and Marc A. Hillmyer^{*}



Cite This: *Biomacromolecules* 2021, 22, 2532–2543



Read Online

ACCESS |



Metrics & More

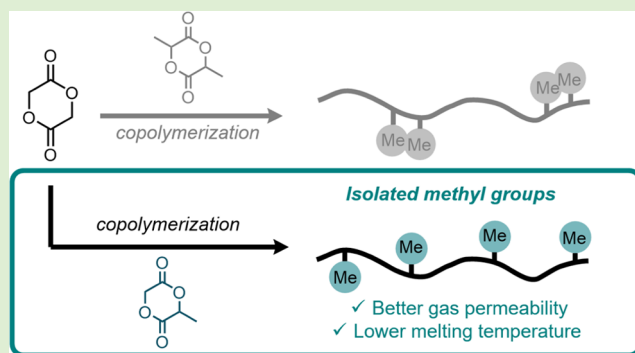


Article Recommendations



Supporting Information

ABSTRACT: An efficient, fast, and reliable method for the synthesis of high-molar-mass polyglycolide (PGA) in bulk using bismuth (III) subsalicylate through ring-opening transesterification polymerization is described. The difference between the crystallization ($T_c \approx 180$ °C)/degradation ($T_d \approx 245$ °C) temperatures and the melting temperature ($T_m \approx 222$ °C) significantly affects the ability to melt-process PGA homopolymer. To expand these windows, the effect of copolymer microstructure differences through incorporation of methyl groups in pairs using lactide or isolated using methyl glycolide ($\leq 10\%$ methyl) as comonomers on the thermal, mechanical, and barrier properties were studied. Structures of copolymers were characterized by nuclear magnetic resonance (^1H and ^{13}C NMR) spectroscopies. Films of copolymers were obtained, and the microstructural and physical properties were analyzed. PGA homopolymers exhibited an approximately 30 °C difference between T_m and T_c , which increased to 68 °C by incorporating up to 10% methyl groups in the chain while maintaining overall thermal stability. Oxygen and water vapor permeation values of solvent-cast nonoriented films of PGA homopolymers were found to be $4.6 \text{ cc}\cdot\text{mil}\cdot\text{m}^{-2}\cdot\text{d}^{-1}\cdot\text{atm}^{-1}$ and $2.6 \text{ g}\cdot\text{mil}\cdot\text{m}^{-2}\cdot\text{d}^{-1}\cdot\text{atm}^{-1}$, respectively. Different methyl distributions in the copolymer sequence, provided through either lactide or methyl glycolide, affected the resulting gas barrier properties. At 10% methyl insertion, using lactide as a comonomer significantly increased both O_2 ($32 \text{ cc}\cdot\text{mil}\cdot\text{m}^{-2}\cdot\text{d}^{-1}\cdot\text{atm}^{-1}$) and water vapor ($12 \text{ g}\cdot\text{mil}\cdot\text{m}^{-2}\cdot\text{d}^{-1}\cdot\text{atm}^{-1}$) permeation. However, when methyl glycolide was utilized for methyl insertion at 10% Me content, excellent barrier properties for both O_2 ($2.9 \text{ cc}\cdot\text{mil}\cdot\text{m}^{-2}\cdot\text{d}^{-1}\cdot\text{atm}^{-1}$) and water vapor ($1.0 \text{ g}\cdot\text{mil}\cdot\text{m}^{-2}\cdot\text{d}^{-1}\cdot\text{atm}^{-1}$) were achieved.



INTRODUCTION

The increase in manufacturing and disposal of synthetic polymers has led to severe polymer pollution, which is an ever-growing concern. One solution to combat global plastic waste is to emphasize, support, and carry out basic research on the development of biobased sustainable polymers as next-generation degradable and compostable materials. Development of biodegradable and biorenewable polymers, such as polyglycolide (PGA) and polylactide (PLA), for use over a wider range of applications and as replacements for petroleum-based synthetic materials has been at the forefront of research efforts.^{1–4} In 2018, a Global Market Insights, Inc. report predicts the value of polyglycolic acid market to be over \$9 billion by 2024. In particular, the medical industry is the largest contributor to this because of the increased use for biomedical applications such as resorbable sutures (e.g., Dexon) and other materials.⁵ Additionally, a significant demand from the packaging industry is expected owing to PGAs low permeability for gases, such as O_2 and CO_2 or water vapor, that is comparable to high-barrier polymers such as ethyl/vinyl alcohol copolymers (EVOH) and poly(vinylidene dichloride) (PVDC).^{6,7}

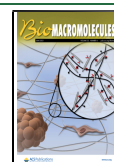
Glycolic acid (GA) is produced from several feedstocks such as formaldehyde and acetic acid, and its synthesis from oxalic acid has also been reported.⁸ GA derived from renewable biomass feedstocks, i.e., glyoxal and dihydroxyacetone, can render it a biorenewable and sustainable monomer.⁹ With the simplest chemical structure among all of the polyesters, PGAs are rigid and highly crystalline (45–55%) thermoplastics. The high gas barrier properties attributed to low free volume, mechanical strength associated with high crystallinity and density, and ease of hydrolytic breakdown and degradation into CO_2 and water in a compost within about a month are all attributes that contribute to the high interest in this material.^{10–19}

A wide variety of synthetic approaches have been reported for the synthesis of PGA homopolymers, including solid-state

Received: March 2, 2021

Revised: April 20, 2021

Published: May 10, 2021



polycondensation of halogenoacetates;^{11,12} synthesis from haloacetic acids,¹³ solution,¹⁴ or melt/solid polycondensation;¹⁵ and alternating copolymerization of C1 feedstocks formaldehyde and carbon monoxide.¹⁶ Ring-opening transesterification polymerization (ROTEP) has been the most commonly used technique for obtaining high-molar-mass PGA-based polyesters. Tin alkoxides and carboxylates are the most widely used catalysts for the synthesis of polyesters and have been employed to obtain PGA molar masses ranging from about 2 to 42 kg·mol⁻¹ in melt polymerizations using 1-dodecanol and 1,4-butanediol as initiators, for example.^{20,21} Recent research has focused on finding new nontoxic metal-based catalysts²² or effective organocatalysts^{23–27} for the polyester synthesis. For example, bismuth salts²⁸ have been employed as catalysts for the copolymerization of glycolide (G) with ϵ -caprolactone (CL)²⁹ and lactides (L)³⁰ but exhibit reduced reactivity compared to typical tin catalysts (e.g., Sn(Oct)₂). Lu et al. reported the synthesis of high-molar-mass PGAs (20–250 kg·mol⁻¹) in bulk at 130–150 °C using diphenyl bismuth bromide.³¹ Chen and co-workers studied the synthesis and catalytic activities of bis(triazol) derivatives of Bi³⁺ complexes with fluorinated and nonfluorinated ligands in the bulk ROP of G and attained high-molar-mass (52 kg·mol⁻¹) PGA homopolymers.³² The melt ring-opening transesterification polymerization of PLAs has been studied using bismuth (III) subsalicylate (BiSS), an effective, relatively low-cost, and commercially available catalyst.³³

Low-molar-mass PGA samples display lower crystallinity, relatively poor thermal and mechanical behavior, and higher water permeability. While high-molar-mass PGA is desirable, high crystallinity leads to low solubility in common solvents, and PGA is only practically soluble in hexafluoroisopropanol (HFIP) and trifluoroacetic acid (TFA). Therefore, PGA homopolymers or copolymers with high PGA content are typically prepared using high-temperature bulk or melt polymerization methods. PGAs can depolymerize at relatively low temperatures ($T_d \approx 245$ °C) following the first-order reaction through intramolecular ester interchange process and release glycolide as the major degradation product.³⁴ PGAs also possess high melting temperatures ($T_m \approx 222$ °C) and high crystallization temperatures ($T_c \approx 180$ °C). The small difference between typical decomposition and melting temperatures can lead to difficulties during the polymerization. Owing to these challenges, studies are limited to some extent regarding the synthesis of PGA homopolymers or copolymers with a high PGA content. Simple and reproducible synthetic methods are desirable for PGA synthesis to produce high-molar-mass samples. Forming robust films also depends on the thermal properties of polymeric samples. As a relatively small difference between T_d and T_m limits the polymer processing due to degradation, the narrow operating window between T_m and T_c can limit melt extrusion processes due to rapid crystallization. Therefore, it is important to expand the window between T_m and T_c and between T_d and T_m by manipulating the chemical structure without compromising the favorable properties of PGA. One way to do this is to introduce a comonomer at a low concentration, which is expected to yield lower T_m and T_c by moderate disruption to the crystal structure.³⁵

We posit that the desirable physical, thermal, and mechanical properties of PGAs can be tuned through low levels of comonomer incorporation while preserving the desirable crystallization and barrier properties of PGAs while

achieving expansion of the thermal processing window. Incorporation of methyl groups in the PGA backbone using lactides has recently been reported, and the thermal, mechanical, and barrier properties of the resultant copolymers were investigated.³⁶ However, the barrier performance of the copolymers was quite diminished compared to PGA. Inspired by the alternating copolymers of lactic acid and glycolic acid synthesized from the ring-opening polymerization of methyl glycolide (MG),^{17,37} we envisioned that insertion of glycolate–lactate–glycolate units into PGA could be carried out using MG and yield samples having improved processability with gas barrier properties similar to PGA. While the use of MG to prepare PLGA block copolymers with ϵ -caprolactone and lactides,³⁸ and star-shaped poly((\pm)-lactic acid-*alt*-glycolic acid), has been investigated,³⁹ the incorporation of MG as a comonomer into PGAs has not been reported. To test our hypothesis, we synthesized PGA homopolymers and its copolymers with either L or MG at low-methyl-group incorporation ($\leq 10\%$) to sufficiently expand the thermal operating window without detrimentally affecting the notable barrier properties of PGAs. Based on nuclear magnetic resonance (NMR) spectra, we demonstrate that copolymers of G with either L or MG reveal different microstructures, and the resultant polymers have been investigated to explore microstructure–property relationships in these new copolymers.

EXPERIMENTAL DETAILS

Materials. Glycolide monomer was purchased from Sigma-Aldrich. It was first recrystallized with activated carbon from ethyl acetate and then recrystallized from ethyl acetate. The glycolide was recrystallized again from dichloromethane and dried in a vacuum oven for 2 days. (\pm)-Lactide was purchased from Sigma-Aldrich. It was recrystallized from toluene three times before polymerization. Bismuth subsalicylate, benzyl alcohol, diphenyl phosphate, and poly(ethylene glycol) (PEG) 600 were purchased from Sigma-Aldrich and used as received. PEG 600 was purged with nitrogen gas in a three-neck round-bottom flask at 60 °C for 3 days to remove any residual water. Hexafluoro-2-isopropanol was obtained from Oakwood Chemical and used as received. Solvents like ethyl acetate and methanol were purchased from Sigma-Aldrich while anhydrous ethyl ether was purchased from Fisher Chemical. They were used as received. Synthesis of *O*-(2-bromopropionyl) glycolic acid and methyl glycolide were synthesized according to literature procedures.⁴⁰

Characterization. ¹H NMR spectra were recorded on a Bruker Advance III HD 400 MHz spectrometer equipped with an autosampler. Chemical shifts are reported in δ units, expressed in ppm using the residual trifluoroacetic acid-*d*₁ signal (11.50 ppm) as an internal standard. Differential scanning calorimetry (DSC) analyses were performed on a TA Instruments Discovery DSC using hermetically sealed aluminum Tzero pans. Scans were conducted under a nitrogen atmosphere at a heating and cooling rate of 10 °C·min⁻¹. Thermogravimetric analysis (TGA) was performed on a TA Instruments Q500 under nitrogen atmosphere at a heating rate of 10 °C·min⁻¹. Size exclusion chromatography (SEC) was performed using a solution of 0.05 M potassium trifluoroacetate in HFIP at a flow rate of 0.35 mL·min⁻¹ and 40 °C on an EcoSEC SEC system HLC-8240GPC series liquid chromatograph fitted with a refractive index detector and two Tosoh TSKgel SuperAWM-H. Molecular masses were determined by conventional calibration using poly(methyl methacrylate) (PMMA) standards. Before SEC analysis, the dissolved polymer was filtered through a 0.2 μ m filter (Whatman) before injection into the column. A polarized optical microscopy (Olympus BX53) equipped with a hot stage (Linkam LTS420E) was used to study the crystallinity and morphologies of neat polymers. Samples were heated to 240 °C and hold for 3 min, then cooled to 25 °C to

crystallize at either 10 or 5 °C·min⁻¹ depending on the composition of the copolymer.

PGA films to test gas permeability were fabricated using a 200 °C Max. Compact Tape Casting Coater with heated vacuum bed (10" W x 16" L) and Doctor Blade-MSK-AFA-H200A. The film-making process was conducted at room temperature and the vacuum was applied. Tensile test for the PGA film was performed using a Shimadzu Autograph AGS-X Tensile Tester. Before the tensile test, the PGA film was made with the thickness ranging from 100 to 200 μm by casting the polymer solution onto glass Petri dishes, followed by drying under ambient conditions and application of vacuum. Water vapor transmission rate (WVTR) studies for the films (having a masked test area of 5 cm²) were carried out with Permatran 3/33 Model G (Mocon) according to ASTM F1249-01 at 90% humidity level, atmospheric pressure, and a temperature of 38 °C. Oxygen transmission rates (OTR) of the films (having a test area of 5 cm² masked) were measured with OxTran 2/21 Model H (Mocon) according to ASTM D3985-02 standard at 0% humidity level with oxygen gas at atmospheric pressure and 23 °C test temperature. Nitrogen gas was used as the carrier gas.

Synthesis of 2-((2-bromopropanoyl)oxy)acetic acid.¹⁹ A round-bottom flask was charged with glycolic acid (23 g, 0.3 mol) in dioxane (110 mL) under an argon atmosphere. 2-Bromopropanoyl bromide (32 mL, 0.31 mol) in dioxane (115 mL) was added slowly at 15 °C for 2 h under Ar. The outlet of the reaction flask was bubbled through the NaOH solution. The reaction mixture was stirred at 15 °C for 2 h, then dioxane was removed in vacuo. The remaining oil was distilled, and the product was collected at 125 °C under 1000 mTorr. The solid was recrystallized from toluene to obtain a white colorless solid. Yield: 20 g (31%). ¹H NMR (CDCl₃, δ, ppm) = 1.88 (3H, -CH₃), 4.47 (1H, -CH); 4.75 (2H, -CH₂) and ¹³C NMR (CDCl₃, δ, ppm) = 21.73 (-CHCH₃), 38.98 (-CHCH₃), 61.13 (-CH₂COOH), 169.78 (-CHCOO-), 172.72 (-COOH).

Synthesis of Methyl Glycolide.¹⁹ A round-bottom flask was charged with NaHCO₃ (2.2 g, 26 mmol) in dimethylformamide (DMF) (150 mL) under an argon atmosphere. 2-((2-bromopropanoyl)oxy)acetic acid (5 g, 24 mmol) in DMF (150 mL) was added slowly for 2 h at 80 °C under Ar. The reaction mixture was stirred at 80 °C for an additional 2 h, then DMF was removed in vacuo. After adding brine, the organic layers were extracted with ethyl acetate. The combined organic layer was dried over MgSO₄, filtered, and concentrated. The crude was recrystallized from ethyl acetate to obtain a colorless solid. Yield: 1.7 g (81%). ¹H NMR (TFA-*d*₁, δ, ppm) = 5.24 (1H, -CHCH₃), 5.09 (2H, -CH₂COO-), 1.69 (3H, -CHCH₃) and ¹³C NMR (TFA-*d*₁, δ, ppm) = 172.73 (-CHCOO-), 170.75 (-CH₂COO-), 77.39 (-CHCH₃), 68.36 (-CH₂COO-); 17.19 (-CH₃).

Example of PGA Homopolymer Synthesis Using Bismuth Subsalicylate (BiSS) Catalyst (14). In an oven-dried 100 mL round-bottom flask containing a magnetic stir bar, glycolide (10 g, 86 mmol), bismuth subsalicylate (3.9 mg, 0.011 mmol), and benzyl alcohol (3.74 μL, 0.036 mmol) with a mole ratio of 2400:0.3:1 were added. Benzyl alcohol (0.187 mL) and toluene (0.813 mL) were added into a small oven-dried vial to make a 1 mL stock solution. The stock solution (20 μL) was taken out and injected into the 100 mL round-bottom flask. The preparation of the reaction was done in a glovebox, and any apparatus used was dried in an oven beforehand to get rid of water vapors. The 100 mL round-bottom flask was sealed with a rubber septum before bringing it out of the glovebox. It was insulated with glass wool and aluminum foil and heated at 230 °C in a heating block for 10 min. After 10 min, the reaction was stopped and allowed to cool to room temperature. The round-bottom flask was then unsealed and an appropriate amount of HFIP was added to dissolve the reaction mixture. When the reaction mixture was fully dissolved in HFIP, it was precipitated into anhydrous ethyl ether (400 mL). The solution was decanted, and the polymer was dried in a vacuum oven overnight. The polymer was refluxed twice using ethyl acetate to remove excess glycolide monomer from the polymer product. Each reflux reaction time was 2 h. Compound 14 had an 82%

conversion, $M_{n,NMR} = 215 \text{ kg}\cdot\text{mol}^{-1}$, $M_{n,SEC} = 91 \text{ kg}\cdot\text{mol}^{-1}$, and $\bar{D} = 2.0$.

Example of PGA Homopolymer Synthesis Using Diphenyl Phosphate (DPP) Catalyst (4). Glycolide (1.5 g, 13.0 mmol), diphenyl phosphate (8.08 mg, 0.032 mmol), and poly(ethylene glycol) (PEG 600) (6.46 mg, 5.72 μL) with a mole ratio of 1200:3:1 were added into an oven-dried vial containing a magnetic stir bar. PEG 600 (5.72 μL) was measured using a microliter syringe and injected into the vial. The preparation of the reaction was done in a glovebox and any apparatus used was dried in an oven beforehand. The vial was capped tightly before being brought out of the glovebox. It was sealed with electrical tape and wrapped with aluminum foil to ensure a constant heat transfer. The vial was heated in a heating block at 200 °C for 2 h. After 2 h, the reaction was stopped and allowed to cool to room temperature. The vial was then unsealed and an appropriate amount of HFIP was added to dissolve the reaction mixture. After the reaction mixture was fully dissolved in HFIP, it was precipitated into diethyl ether (100 mL). The solution was decanted, and the polymer was dried in a vacuum oven overnight. The polymer was refluxed twice using ethyl acetate at 88 °C and each reflux reaction time was 2 h. Compound 4 had a 25% conv. $M_{n,NMR} = 29 \text{ kg}\cdot\text{mol}^{-1}$, $M_{n,SEC} = 19 \text{ kg}\cdot\text{mol}^{-1}$ and $\bar{D} = 1.7$.

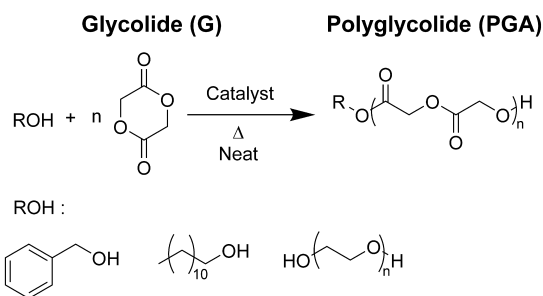
Example of Preparation of Thin Films Using Lower-Molar-Mass PGAs (30k–40k). In a 20 mL scintillation vial, 650 mg of PGA beads was first dissolved in 7.31 mL of HFIP to make a solution with a concentration of 5 wt % in HFIP. The vial was heated in a heating block at 50 °C until the polymer was completely dissolved in the HFIP. A magnetic stir bar and 2.44 mL of HFIP were then added into the vial to decrease the concentration of the solution to 4.0 wt % in HFIP. The vial was placed on a magnetic stirrer without heating it and allowed for a homogeneous solution to form. The solution was filtered through a 0.45 μm polypropylene filter and ready for film making. On a tape casting coater, a piece of aluminum foil was placed underneath a fluorinated ethylene propylene (FEP) film on the surface of the coater. The coater was set at room temperature, the height of the applicator was set at 0.345 mm, and the speed of the applicator was set at 50 mm/s. A small amount of isopropanol was sprayed on the FEP surface and wiped using a piece of Kimwipe before pouring the polymer solution on it. The solution was poured evenly on the FEP surface and an inch off from the edges of the applicator to avoid accumulation of solution at the sides of the film. Once the vacuum was applied, the applicator was started to push the polymer solution and spread it to form a uniform surface and thickness. Tweezers were used to peel the PGA film off from the FEP film as it would stick on the surface even when it dried out. A micrometer screw gauge was used to measure the thickness of the PGA film.

Example for Preparation of Thin Film Using Higher-Molar-Mass PGAs (>40k). In a 20 mL scintillation vial, 802 mg of PGA beads was first dissolved in 9.02 mL of HFIP to create a polymer solution with a concentration of 5.3 wt % in HFIP. The vial was heated in a heating block at 50 °C until the polymer beads were completely dissolved in HFIP. HFIP (1.03 mL) and isopropanol (IPA, 0.26 mL) were then added into the vial. A polymer solution with a concentration of 4.5 wt % in HFIP and 2.5 vol % of IPA was made. A magnetic stir bar was also put into the vial. The vial was placed on the magnetic stirrer without heating it until a homogeneous solution was formed. The polymer solution was filtered through a 0.45 μm polypropylene filter and ready for film making. On a tape casting coater, a piece of aluminum foil was placed underneath a FEP film on the surface of the coater. The coater was set at room temperature, the height of the applicator was set at 0.25 mm, and the speed of the applicator was set at 50 mm·s⁻¹. The polymer solution was poured evenly. The applicator was started to push and spread the polymer solution on the FEP film surface after the vacuum was applied. When the PGA film was dried out, it would peel off by itself from the FEP film. The thickness of the PGA film was measured using a micrometer screw gauge.

RESULTS AND DISCUSSION

ROTEP Synthesis of PGA Homopolymers. Bulk polymerization of G was studied using various catalysts to identify the optimal conditions for the preparation of high-molar-mass PGAs through ROTEP (Scheme 1). Acid-catalyzed (diphenyl phosphate) and metal-catalyzed ($\text{Sn}(\text{Oct})_2$ and BiSS) bulk homopolymerizations of G were investigated (Table 1).

Scheme 1. ROTEP Synthesis of Polyglycolide Using ROH Initiators



Diphenyl phosphate (DPP) is an effective organocatalyst for ROTEP of cyclic esters.^{26,41} Liu et al. reported polymerization of ϵ -caprolactone, δ -valerolactone, and (-)-lactide with high conversion at 180 °C in bulk using DPP at an equimolar ratio of catalyst to initiator.⁴² However, this method has not been reported previously for the synthesis of PGAs. Initially, G was polymerized in bulk using DPP as a catalyst and benzyl alcohol as an initiator at 200 °C, which resulted in 99% conversion after 2 h ($M_{n,\text{SEC}} = 7.8 \text{ kg}\cdot\text{mol}^{-1}$) (Table 1; 1). The relative molar mass by SEC analysis (vs PMMA standards) was similar to the molar mass by ¹H NMR spectroscopic analysis with $M_{n,\text{NMR}}$ obtained by comparing the peak from the BnOH end group at 7.3 ppm to the methylene peak of PGA at 5.0 ppm (Figure S1). Bulk polymerizations at higher monomer-to-initiator ($[\text{M}]_0/[\text{I}]_0$) ratios gave insoluble products. ROTEP synthesis of PGA at $[\text{M}]_0/[\text{I}]_0 = 100$ afforded quantitative

conversion (99%) ($M_{n,\text{SEC}} = 12 \text{ kg}\cdot\text{mol}^{-1}$, 2) when PEG 400 was employed as an initiator (Figure S2), and homopolymers with molar masses reaching up to 15 $\text{kg}\cdot\text{mol}^{-1}$ (3) and dispersity values below 2 were obtained within a few hours. However, at higher $[\text{M}]_0/[\text{I}]_0$ ratios, it proved difficult to achieve high conversion, and increasing the catalyst loading and reaction times might result in degradation (Figure S3C).

$\text{Sn}(\text{Oct})_2$ is a thermally stable catalyst, which is widely used for bulk polymerization of cyclic esters at high temperatures.^{20,43,44} At 230 °C, $\text{Sn}(\text{Oct})_2$ mediated the rapid polymerization of G (3 min) using benzyl alcohol as an initiator at $[\text{M}]_0/[\text{I}]_0 = 100$, thereby generating polyglycolide of 14 $\text{kg}\cdot\text{mol}^{-1}$ with 92% conversion (Table 1; 5). Increasing $[\text{M}]_0/[\text{I}]_0$ ratio to 300 resulted in higher-molar-mass (23 $\text{kg}\cdot\text{mol}^{-1}$) polymer (Table 1; 6). However, even higher molar masses could not be achieved, even with an $[\text{M}]_0/[\text{I}]_0$ ratio of 600 (Table 1; 7). Additionally, $M_{n,\text{SEC}}$ (16 $\text{kg}\cdot\text{mol}^{-1}$) deviated from $M_{n,\text{NMR}}$ (70 $\text{kg}\cdot\text{mol}^{-1}$), suggesting fortuitous initiation by water. Due to the lack of success in preparing polymer samples with reproducible and high molar masses, the resulting large dispersities, and pale brown products, $\text{Sn}(\text{Oct})_2$ was not a practical catalyst in our hands for the synthesis of high-molar-mass PGA samples under the conditions we explored.

ROTEP synthesis of PGA in bulk was also performed using BiSS as a catalyst and BnOH as an initiator at 230 °C under an inert atmosphere (Table 1). Using a 0.03 catalyst-to-initiator ratio ($[\text{C}]_0/[\text{I}]_0$) resulted in a low conversion (13%) and a low $M_{n,\text{SEC}}$ (9 $\text{kg}\cdot\text{mol}^{-1}$) (Table S1; s1). Increasing $[\text{C}]_0/[\text{I}]_0$ to 0.1 provided higher conversion (99%) and higher $M_{n,\text{SEC}}$ (20 $\text{kg}\cdot\text{mol}^{-1}$), but high dispersity values ($\mathcal{D} = 3.3$) (Table S1; s2). As we increased the $[\text{C}]_0/[\text{I}]_0$ ratio from 0.1 to 0.3, the dispersities decreased from 3.3 to 1.9 and molar masses increased to 49 $\text{kg}\cdot\text{mol}^{-1}$ (Table S1; 9). At even higher $[\text{C}]_0/[\text{I}]_0$ ratios (0.6–1.8), however, a slight increase in dispersity was observed in conjunction with a decrease in molar mass (Table S1; s5–s7). Considering the conversion, molar mass, and dispersities, the optimum $[\text{C}]_0/[\text{I}]_0$ was determined to be 0.3 (Figure 1A), or about 3 initiator molecules for every catalyst molecule. The optimal reaction time for BiSS-catalyzed

Table 1. ROTEP Synthesis of Polyglycolide

sample ID	C	mole ratios			T (°C)	time (min)	conv ^a (%)	$M_{n,\text{theo}}$ ($\text{kg}\cdot\text{mol}^{-1}$)	$M_{n,\text{NMR}}$ ^a ($\text{kg}\cdot\text{mol}^{-1}$)	$M_{n,\text{SEC}}$ ^b ($\text{kg}\cdot\text{mol}^{-1}$)	\mathcal{D} ^b
		M	C	I							
1	DPP	67	0.3	1	200	120	99	7.7	9.1	7.8	2.2
2 ^c	DPP	100	1	1	200	120	99	12	11	12	2.0
3 ^d	DPP	300	1	1	200	180	53	18	14	15	2.0
4 ^d	DPP	1200	3	1	200	480	25	34	29	19	1.7
5 ^e	$\text{Sn}(\text{Oct})_2$	100	0.006	1	230	3	92	11	9.9	14	2.8
6 ^e	$\text{Sn}(\text{Oct})_2$	300	0.006	1	230	30	85	30	40	23	3.6
7 ^e	$\text{Sn}(\text{Oct})_2$	600	0.006	1	230	60	85	59	70	16	3.4
8 ^e	BiSS	100	0.3	1	230	10	97	11	14	13	2.7
9 ^e	BiSS	300	0.3	1	230	10	94	33	40	49	1.9
10 ^e	BiSS	600	0.3	1	230	10	98	68	71	74	1.9
11 ^e	BiSS	900	0.3	1	230	10	98	102	121	86	2.0
12 ^f	BiSS	900	0.3	1	230	10	98	102	63	96	1.9
13 ^e	BiSS	1200	0.3	1	230	10	94	131	134	69	2.0
14 ^e	BiSS	2400	0.3	1	230	10	82	230	215	91	2.0
15 ^e	BiSS	3600	0.6	1	230	10	89	371	369	92	2.0
16 ^e	BiSS	4800	1.0	1	230	10	96	532	497	108	1.9

^aDetermined by the internal standard method with alcohol based on ¹H NMR spectroscopy. ^bObtained by HFIP SEC using PMMA calibration. ^cInitiator: PEG 400. ^dInitiator: PEG 600. ^eInitiator: BnOH. ^fInitiator: 1-dodecanol.

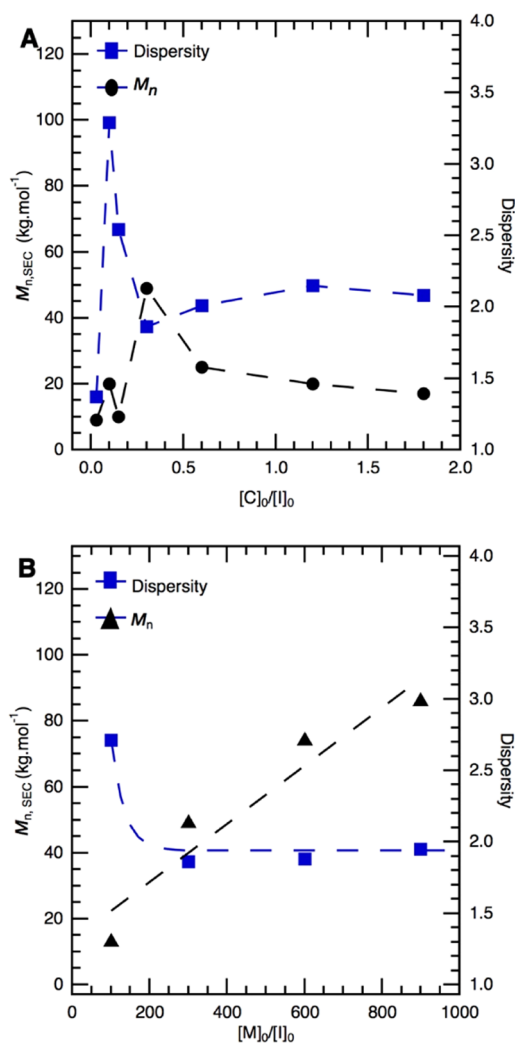


Figure 1. Plots for the ROTEP synthesis of PGA homopolymers prepared in bulk at 230 °C in 10 min using BiSS as a catalyst. (A) $M_{n,SEC}$ and dispersity as a function of $[C]_0/[I]_0$ at $[M]_0/[I]_0 = 300$. (B) $M_{n,SEC}$ and dispersity against $[M]_0/[I]_0$ at $[C]_0/[I]_0 = 0.3$.

polymerizations was found to be 10 min at 230 °C to obtain high conversions. As expected, shorter reaction times resulted in lower conversion (25% after 5 min; Table S1, s4) and a slight discoloration of products was observed at 30 min. Polymerizations using the optimized $[C]_0/[I]_0$ ratio, reaction

temperature, and reaction time were performed well to give a linear increase in $M_{n,SEC}$ with increasing $[M]_0/[I]_0$ from 100 to 900 at a constant $[C]_0/[I]_0$ and near-constant conversion (Table 1; 8–11 and Figure 1B). Monomodal distributions were observed for the polymers based on SEC analysis (Figure S4A). Furthermore, $M_{n,SEC}$ (vs PMMA standards) was in good agreement with $M_{n,NMR}$, consistent with the polymerizations being largely initiated by BnOH. However, a higher molar mass of polymer was not obtained upon further increasing $[M]_0/[I]_0$ to 1200 and 2400, presumably due to the presence of fortuitous initiator (e.g., low levels of water) (Table 1; 13, 14). To achieve higher-molar-mass polymers, polymerization at an even higher $[C]_0/[I]_0$ ratio was performed and provided $M_{n,SEC} = 108 \text{ kg}\cdot\text{mol}^{-1}$ (Table 1; 16). ROTEP of G was also performed in the absence of an alcohol initiator (Table S1; s9); however, the polymerization in the presence of benzyl alcohol was more controlled and yielded lower-dispersity product (Table S1; s8). When BnOH was replaced with 1-dodecanol (Table 1; 12) as a higher-boiling point alcohol to initiate the polymerization, a similar $M_{n,SEC}$ value was obtained. Regardless of the reaction conditions, all polymers prepared at 230 °C in 10 min using BiSS as a catalyst yielded white powders upon precipitation from HFIP into cold diethyl ether. BiSS proved to be a superior catalyst for bulk polymerization of G and was employed to synthesize the target copolymers.

Copolymerization of Glycolide with Lactide or Methyl Glycolide Using BiSS. Racemic (\pm)-lactide (L) or (\pm)-methyl glycolide (MG) was copolymerized with glycolide (G) using BiSS as a catalyst (Scheme 2). To keep the methyl content low, a maximum of 10–20% mole fraction of L or MG in the feed was employed (Table 2). Copolymerizations of G and L in bulk for 10 min using BnOH as an initiator resulted in poly(glycolide-*stat*-((\pm)-lactide)) (PGL) molar masses from 22 to 102 $\text{kg}\cdot\text{mol}^{-1}$ at high conversions and dispersities less than 2. Copolymerization of L and G can be conducted at temperatures lower than 230 °C due to the reduced T_m values of copolymers. Therefore, PGL syntheses were performed at 180–220 °C. The level of incorporated methyl groups was calculated from ¹H NMR analysis based on methylene peaks (5.00 ppm) of PGA units and methyl peaks of PLA units (1.64 ppm) in the resulting polymers (Figure S5) and found within the range of 4–10% (Table 2; PGL1–PGL6).

Likewise, poly(glycolide-*stat*-((\pm)-methyl glycolide)) (PGMG) was prepared by varying the $[M]_0/[I]_0$ ratio using 10 and 20% mole fractions of MG in the feed (Table 2). The bulk copolymerization with $[M]_0/[I]_0$ of 500:1 with 10% feed

Scheme 2. Copolymerization of Glycolide with (\pm)-Lactide or (\pm)-Methyl Glycolide Using BiSS

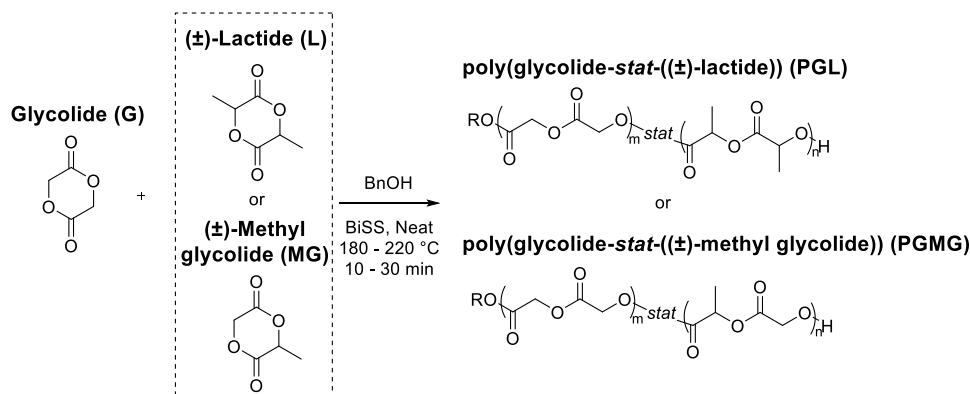


Table 2. Polymerization of Glycolide with (±)-Lactide or (±)-Methyl Glycolide Using BiSS^a

sample ID	[G] ₀ to [L] ₀ or [MG] ₀	mole ratios			T (°C)	time (min)	conv. ^b (%)	M _{n,theo} ^c (kg/mol)	M _{n,NMR} ^d (kg/mol)	M _{n,SEC} ^e (kg/mol)	Đ ^f	Me ^g (%)
		M	C	BnOH								
PGL1	90:10	100	0.3	1	210	10	97	11	30	22	1.8	8
PGL2	90:10	500	0.3	1	210	10	94	55	57	73	1.8	8
PGL3	90:10	1000	0.3	1	210	10	85	101	139	102	1.7	4
PGL4	85:15	900	0.3	1	220	10	90	92	100	86	1.9	10
PGL5	85:15	1200	0.3	1	220	10	77	111	119	81	1.8	6
PGL6	85:15	900	0.3	1	180	10	92	98	116	108	2.0	10
PGMG1	90:10	500	0.3	1	210	20	97	57	10	34	2.3	5
PGMG2	90:10	500	0.3	1	210	30	98	59	14	17	3.0	4
PGMG3	90:10	1000	0.3	1	210	20	87	102	30	55	2.6	5
PGMG4	90:10	1500	0.3	1	210	20	85	150	27	81	1.9	4
PGMG5	90:10	2000	0.3	1	210	20	72	169	13	39	2.3	4
PGMG6	80:20	500	0.3	1	210	20	97	58	21	27	2.4	10
PGMG7	80:20	1000	0.3	1	210	20	86	102	31	46	2.5	9
PGMG8	80:20	1000	0.3	1	180	20	84	99	19	33	2.3	8
PGMG9	80:20	1000	0.3	1	180	30	93	111	19	46	2.3	9
PGMG10	80:20	2000	0.3	1	180	20	80	188	10	34	2.1	8

^aPolymerizations were performed in bulk. ^bNormalized average with mole ratio of conv_G and conv_{CM} determined by ¹H NMR spectroscopy. ^cCalculated by $([M_G]/[I]) \times \text{conv}_G \times \text{MW}_G + ([M_{CM}]/[I]) \times \text{conv}_{CM} \times \text{MW}_{CM}$. ^dDetermined by ¹H NMR spectroscopy. ^eDetermined by HFIP SEC calibrated using PMMA standard. ^fMethyl incorporation in the polymer backbone calculated by the number of methyl group divided by the sum of the number of methylene and methyl group based on ¹H NMR spectroscopy. CM: (±)-methyl glycolide or (±)-lactide.

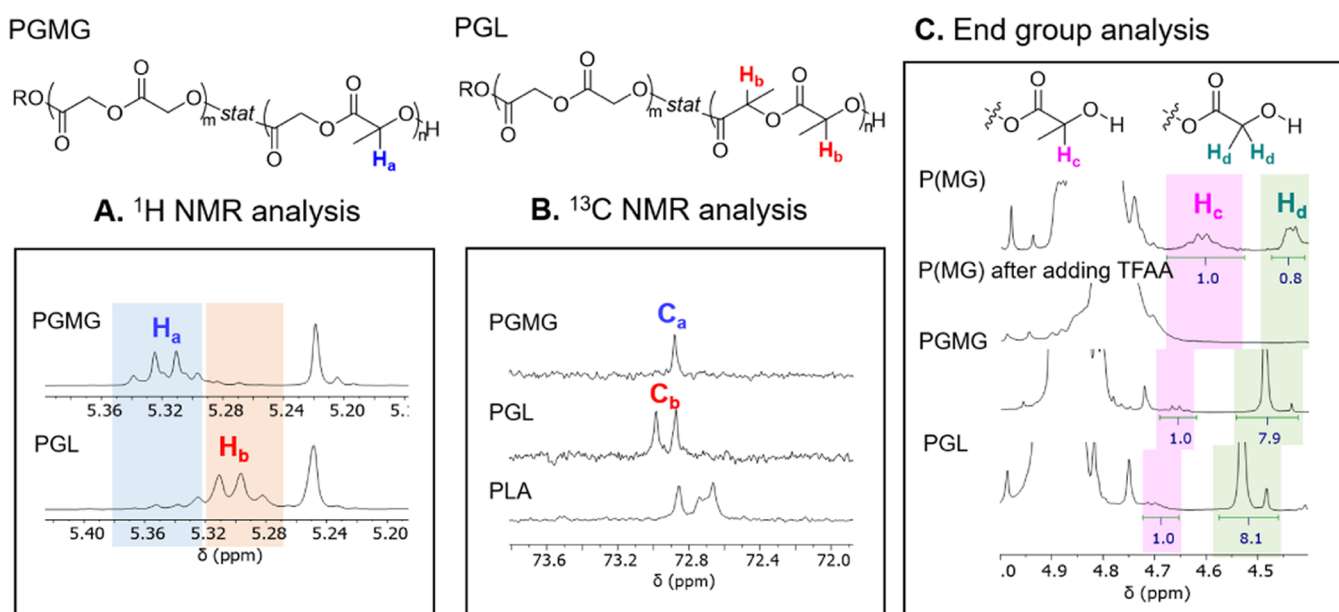


Figure 2. (A) ¹H NMR analysis of PGMG (2.5 kg·mol⁻¹, 9% methyl group in the polymer backbone) and PGL (2.6 kg·mol⁻¹, 9% of methyl group in the polymer backbone) in TFA-*d*₁ and CDCl₃. (B) ¹³C NMR analysis of PGMG, PGL, and PLA (4.9 kg·mol⁻¹) in TFA-*d*₁ and CDCl₃. (C) End group analysis of the P(MG) (2.5 kg·mol⁻¹), PGMG, and PGL in TFA-*d*₁ and CDCl₃.

composition of MG at 210 °C consumed monomer rapidly (97% conversion within 20 min), producing PGMG of $M_n = 34 \text{ kg}\cdot\text{mol}^{-1}$ (Table 2; PGMG1). While 10 mol % L feed was expected to result in 10% methyl group content in the backbone for PGL, 5% methyl group content was expected when 10 mol % MG feed was used. Based on ¹H NMR analysis, 10% feed mole fraction of MG resulted in 5% methyl incorporation in the backbone as expected (Table 2; PGMG1). However, unlike MG, L incorporation deviated from the L feed ratio, resulting only in 8% incorporation (Table 2; PGL1). This observation may be due to the lower overall steric hindrance in MG as compared to L (Table 2;

PGL1 and PGMG1) during propagation. For longer reaction times (30 min), the polymerizations resulted in the PGMG with decreased molar mass ($M_n = 17 \text{ kg}\cdot\text{mol}^{-1}$) possibly because of intramolecular transesterification (Table 2; PGMG2). Higher-molar-masses of PGMG were achieved by increasing the $[M]_0/[I]_0$ ratio with 4–5% of methyl group incorporation (Table 2; PGMG3–PGMG5). For high-molar-mass samples ($M_{n,SEC} = 81 \text{ kg}\cdot\text{mol}^{-1}$), however, the molar mass obtained by ¹H NMR analysis deviated from the value obtained by the SEC because of the technical difficulty of the end group analysis by NMR spectroscopy. Using a 20% feed ratio of MG, a variety of molar masses were obtained by

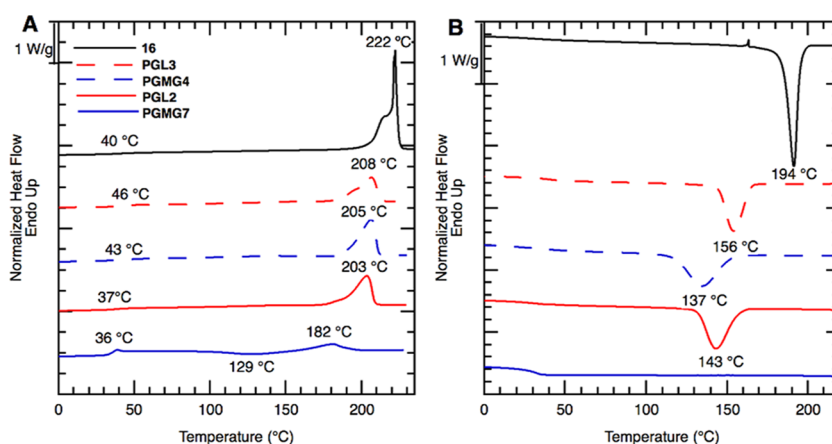


Figure 3. DSC analysis of **16** (108k, 0% Me), **PGL3** (102k, 4% Me), **PGMG4** (81k, 4% Me), **PGL2** (73k, 8% Me), and **PGMG7** (46k, 9% Me) under $N_{2(g)}$ atmosphere. (A) Determined at a heating rate of $10\text{ }^{\circ}\text{C}\cdot\text{min}^{-1}$ based on the second heating cycle. (B) Determined at a cooling rate of $10\text{ }^{\circ}\text{C}\cdot\text{min}^{-1}$ based on the first cooling cycle.

Table 3. Thermal Properties of PGA and Copolymers Prepared Using BiSS

sample ID	^a		TGA ^c		DSC ^d			
	% Me ^a	$M_{n,SEC}$ ^b (kg·mol ⁻¹)	$T_{d,5wt\%}$ (°C)	T_g (°C)	T_m (°C)	ΔH_m ^e (J/g)	T_c^f (°C)	χ_c^g (%)
s1	0	9	275	broad	212	85	185	41
13	0	69	302	37	222	90	195	44
16	0	108	298	37	222	93	194	45
PGL3	4	102	272	46	208	51	156	25
PGMG4	4	81	294	43	205	65	137	31
PGL2	8	73	246	38	203	57	143	28
PGMG7	9	46	260	36	182	23	129 ^h	11

^aMethyl incorporation in the polymer backbone calculated by the number of methyl group divided by the sum of the number of methylene and methyl group based on ^1H NMR spectroscopy. ^bDetermined by HFIP SEC calibrated using PMMA standards. ^cDetermined by TGA at a heating rate of $10\text{ }^{\circ}\text{C}/\text{min}$ under nitrogen atmosphere. ^dDetermined by DSC analysis under N_2 atmosphere at a heating and cooling rate of $10\text{ }^{\circ}\text{C}/\text{min}$ based on the second heating cycle. ^e ΔH_m was determined based on the second heating cycle. ^fDetermined by DSC analysis under N_2 atmosphere at a cooling rate of $10\text{ }^{\circ}\text{C}/\text{min}$ based on the first cooling cycle. ^gPercent crystallization (%) was calculated by $\chi_c (\%) = [(\Delta H/\Delta H_0) \times 100]$, where $\Delta H_0 = 206.4\text{ J/g}$. ^hDetermined by DSC analysis under N_2 atmosphere at a heating rate of $10\text{ }^{\circ}\text{C}/\text{min}$ based on the second heating cycle because T_c was not observed in the first cooling cycle.

varying $[M]_0/[I]_0$ ratio from 500 to 2000 with 8–10% methyl incorporation in the polymer backbone (Table 2; PGMG6–PGMG10). Notably, $180\text{ }^{\circ}\text{C}$ was a high enough temperature for melt polymerization due to the low melting temperature of the resulting copolymers. These experiments highlighted that molar masses and methyl incorporation of polymers can be controlled by $[M]_0/[I]_0$ ratio and mole fraction of MG, respectively.

^1H NMR, ^{13}C NMR, and heteronuclear multiple bond correlation (HMBC) spectroscopies were used to investigate detailed chemical structures and microstructures of polymers. To analyze end groups of the polymers, low-molar-mass PGA and copolymers were synthesized. In the ^1H NMR spectrum, PGA backbone peak appeared at 5.09 ppm in TFA- d_1 (Figure S7). The methylene protons adjacent to the terminal hydroxyl group were clearly identified as the peak at 4.66 ppm was shifted to 5.05 ppm (Figure S1) by the addition of trifluoroacetic anhydride (TFAA) resulting in the putative formation of the trifluoroacetate end group. The other end group peaks at 5.01 and 5.39 ppm correlated with benzyloxy carbonyl and phenyl groups by HMBC analysis, respectively, suggesting that they were from the end group as a result of BnOH initiation (Figure S7). ^1H NMR spectra of PGL and PGMG showed methyl (1.6 ppm) and methine protons (5.3 ppm) in addition to PGA backbone methylene (Figures 2, S5,

and S6) peaks. For ^{13}C NMR spectra, two and one methine carbon peaks appeared for PGL and PGMG, respectively, while PLA had more than three methine carbon peaks. This data suggested that PGL and PGMG had glycolate–lactate–lactate–glycolate and glycolate–lactate–glycolate sequences, respectively, without significant levels of blocky PLA sequences (Figure 2B). The ^1H NMR spectra showed methine protons in PGMG (H_a) and PGL (H_b) that exhibited slightly different chemical shifts at 5.32 and 5.30 ppm, respectively (Figure 2A). ^1H NMR and ^{13}C NMR spectroscopies indicated that PGL and PGMG have distinct methyl group distributions, as expected.

To analyze end groups and elucidate the reactive site of MG, an oligomer of P(MG) ($2.5\text{ kg}\cdot\text{mol}^{-1}$) was synthesized. The end groups of methine protons (H_c) and methylene protons (H_d) adjacent to the hydroxyl group appeared at 4.61 and 4.40–4.56 ppm, respectively, supported by adding TFAA (Figure 2C). The integration of H_c was 71% compared to sum of H_c and H_d , suggesting that sterically less hindered carbonyl of MG is more likely to react with the alcohol propagating group than more hindered carbonyl site.^{17–19,45} In this regard, when 20% of MG was incorporated to PGA, we anticipated that PGMG would have 14% ($20\% \times 71\%$) of H_c as an end group. In fact, the integration of H_c in PGMG was 20%, suggesting that methyl groups were likely distributed

essentially randomly with slight enrichment at the end of polymer chains. The consecutive lactate-lactate sequence was also incorporated slightly more at the end of the PGL chains, supported by the integration of methylene and methine protons in the end groups.

Thermal Properties of PGA Homopolymers and Copolymers. Thermogravimetric analysis (TGA) and differential scanning calorimetry (DSC) were used to investigate the thermal properties of PGA homopolymers and copolymers (Figure 3 and Table 3). The thermal decomposition of PGAs as characterized by the 5% mass loss ($T_{d,5\%}$) values measured at a rate of $10\text{ }^{\circ}\text{C}\cdot\text{min}^{-1}$ under nitrogen was in the range of 275–302 $^{\circ}\text{C}$. PGA prepared using DPP (Table 1; 3) displayed $T_{d,5\%}$ at 321 $^{\circ}\text{C}$, which was higher than the $T_{d,5\%}$ values of homopolymer samples obtained using either BiSS or Sn(Oct)₂. The residual DPP catalyst (0.001–5 wt %) possibly acts as a thermal stabilizer in these cases.⁴⁶ The glass-transition temperature (T_g) for PGA was observed at 37 $^{\circ}\text{C}$ (Table 3; 13 and 16) but was not observed for low-molar-mass PGA sample ($9\text{ kg}\cdot\text{mol}^{-1}$) (Table 3; s1). The melting (T_m) and the crystallization (T_c) temperatures showed a slight variation ranging from 212 to 222 $^{\circ}\text{C}$ and 185 to 195 $^{\circ}\text{C}$, respectively (Figure 3, black line and Table 3). The thermal properties obtained for PGA samples were in good agreement with previous studies.⁴⁷

Derivative thermogravimetry results showed one-step decomposition for PGA and PGL, but two-step decomposition was observed for PGMG. The copolymers thermally degraded at similar temperatures as the PGA homopolymers. The resulting PGMG and PGL polymers exhibited a 5% mass loss at 246–294 $^{\circ}\text{C}$ (Table 3 and Figure S8). Notably, the difference between the thermal decomposition and melting temperature ($T_{d,5\%}-T_m$) is an important property for melt processing applications, as it forms a range of suitable temperatures at which the polymer can be processed without substantive degradation due to mass loss. Thus, it is worth noting that $T_{d,5\%}-T_m$ increased up to 89 $^{\circ}\text{C}$ (Table 3; PGMG4) when methyl groups were incorporated, compared to high-molar-mass PGA homopolymer samples (76 $^{\circ}\text{C}$, Table 3, 16). At a low level of Me group incorporation, T_m reduced from 222 to 205 $^{\circ}\text{C}$ and χ_c reduced from 45 to 25% consistent with the fact that even a small amount of methyl groups can act as defects thwarting crystallization. Interestingly, PGL and PGMG had different thermal properties even with similar methyl group contents. PGL with 8% methyl group exhibited T_m at 203 $^{\circ}\text{C}$ with 28% crystallinity (Table 3; PGL2) and no cold crystallization peak, while PGMG with 9% Me showed T_m at 182 $^{\circ}\text{C}$ with 11% crystallinity and T_{cc} at 129 $^{\circ}\text{C}$ (Table 3; PGMG7) when measured at a cooling rate of $10\text{ }^{\circ}\text{C}\cdot\text{min}^{-1}$. The difference between T_m and T_c is also an important value for extrusion of films and sheets because fast crystallization upon cooling can limit processing protocols. PGA has a relatively small T_m-T_c difference (28 $^{\circ}\text{C}$); thus, it can be challenging to prepare films and sheets through extrusion.⁴⁸ Incorporation of methyl groups is advantageous in this regard, as the decreased crystallization temperatures (T_c), allowed for larger T_m-T_c in the range from 52 to 68 $^{\circ}\text{C}$ (Figure 3). Surprisingly, PGMG with 9% methyl incorporation did not show a crystallization peak in the cooling cycle, presumably due to slow crystallization, while PGL with 8% methyl incorporation revealed a crystallization exotherm centered at 143 $^{\circ}\text{C}$. The thermal analysis indicates that different methyl distributions from lactide or methyl glycolide induced different

thermal properties and crystallization behavior, even with a similar level of methyl incorporation.

Crystalline Structures of PGA Homopolymers and Copolymers. Crystalline structures of PGA, PGL, and PGMG were investigated using wide-angle X-ray diffractometry (WAXD). WAXD data of solvent-cast films were recorded at 25 $^{\circ}\text{C}$ using a Bruker Discover D8 instrument equipped with a Co-K α source ($\lambda = 1.79\text{ \AA}$). PGA showed diffraction peaks at 25.7 and 33.4 $^{\circ}$, which are attributed to the (110) and (020) crystalline planes, respectively (Figure 4).⁴⁹ Interplanar

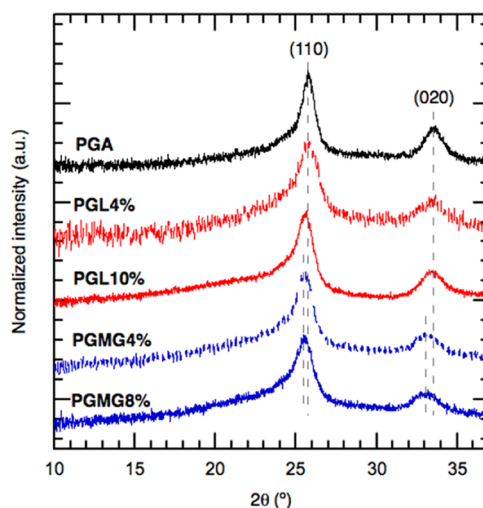


Figure 4. WAXD profiles of PGA (11, 86k), PGL4% (PGL3, 102k), PGL10% (PGL4, 86k), PGMG4% (PGMG4, 81k), and PGMG8% (PGMG10, 34k). Gray dash lines are the main diffraction angles.

distances (d) of PGA and PGL were obtained from WAXD profile, resulting in 4.02 and 3.11 \AA for (110) and (020) planes, respectively. These values agree with previous studies.⁴⁹ PGL had similar diffraction peaks compared to PGA at 25.8 and 33.6 $^{\circ}$ for (110) and (020), respectively, suggesting that (\pm)-lactide units act as defects that were not incorporated into the crystal lattice. This trend was different from earlier studies that concluded (–)-lactic acid co-crystallized with glycolic acid in poly(glycolic acid-*stat*-((–)-lactic acid)), presumably due to the stereo-irregularity and different microstructure of PGL in our case.⁴⁹ Interestingly, diffraction peaks of PGMG appeared at 25.5 and 32.8 $^{\circ}$ for (110) and (020) planes, respectively, which were slightly shifted to lower angles compared to PGA and PGL. The d values of PGMG were 4.06 and 3.17 \AA for (110) and (020) planes, respectively. Similar results have been found in the previous studies of poly(glycolic acid-*stat*-((–)-lactic acid)). It was stated that higher d values of copolymers than PGA suggested co-crystallization of glycolic acid and (–)-lactic acid units in the crystalline lattices.

The effects of L or MG insertion on the spherulite growth behavior were also investigated through nonisothermal crystallization using polarized optical microscopy. Figure 5 shows the photomicrographs of neat PGL and PGMG taken during the cooling from molten state at 240 $^{\circ}\text{C}$. Copolymer film samples were ramped to 240 $^{\circ}\text{C}$ at a rate of $30\text{ }^{\circ}\text{C}\cdot\text{min}^{-1}$ and held at this temperature for 3 min. Then, the temperature was reduced to 25 $^{\circ}\text{C}$ at a cooling rate of $10\text{ }^{\circ}\text{C}\cdot\text{min}^{-1}$ and the crystal formation of PGL and PGMG copolymers was recorded during the cooling process. The spherulites for both PGL_{4%} and PGMG_{4%} began to appear at 169 $^{\circ}\text{C}$. When the

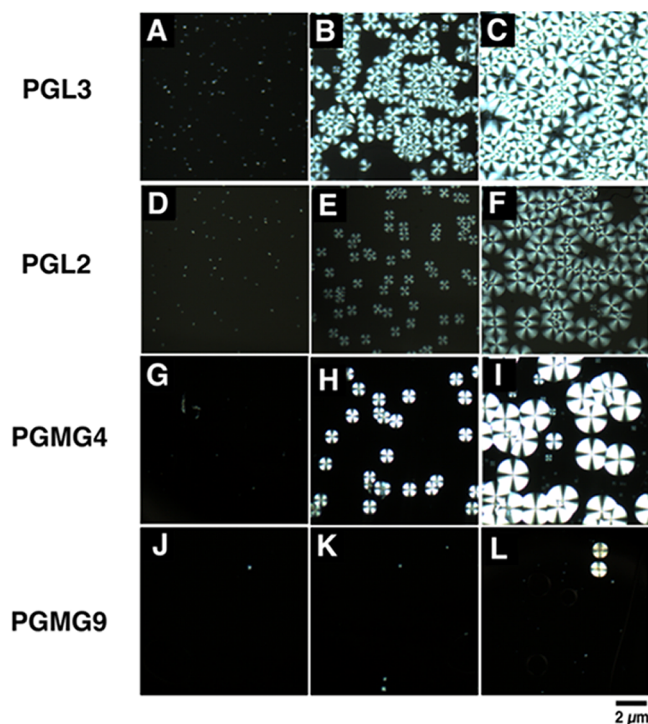


Figure 5. Polarized optical micrographs of copolymers recorded at various temperatures: PGL3 (4% Me) at: (A) 169 °C, (B) 140 °C, and (C) 100 °C; PGL2 (8% Me) at: (D) 160 °C, (E) 140 °C, and (F) 100 °C; PMMG4 (4% Me) at: (G) 169 °C, (H) 140 °C, and (I) 100 °C; and PMMG9 (9% Me) at: (J) 106 °C, (K) 96 °C, and (L) 61 °C.

temperature was reduced to 140 °C, the area covered with crystals was larger for PGL_{4%} than PMMG_{4%}, but their spherulite sizes were similar. An increase in spherulite size was observed for PMMG_{4%} as the temperature reduced from 140 to 100 °C. The same temperature decrease did not profoundly affect the size of PGL_{4%} spherulites. The crystal formation for PMMG_{9%} was too slow at 10 °C·min⁻¹; therefore, we utilized a slower cooling rate of 5 °C·min⁻¹. Increasing the amount of % Me to 9% using MG reduced both the growth rate and T_c . PMMG_{9%} started to form crystals at 106 °C. The data support the DSC results, where incorporating 9% Me using MG significantly reduced the rate of crystal formation. Also, the size and the area covered with crystals significantly reduced.

Mechanical Properties. Tensile tests were performed to investigate the mechanical properties of PGA homopolymers and copolymers. Samples were solvent-cast from HFIP, dried for more than 1 day, and cut into dog-bone test shapes. Representative data sets are shown in Figure 6 and Table S3. PGA and copolymers had Young's moduli in the range from 0.46 to 1.0 GPa. PGA exhibited brittle fracture with an ultimate tensile strength of 12 MPa and an elongation at break of 4.5% due to the high crystallinity of the material. These values are lower than commercial PGA (Kuredux) prepared by injection molding with a high tensile strength of 117 MPa and an elongation at break of 13%, as reported by Kureha, presumably due to the higher degree of chain alignment and crystallinity from different processing conditions.⁵⁰ The copolymers showed ultimate tensile strengths up to 12 MPa and 8% strains at break. Interestingly, PMMG with 9% Me slightly outperformed the other polymers with respect to

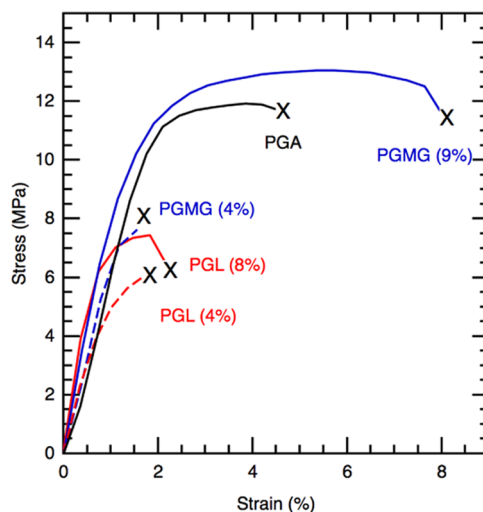


Figure 6. Representative uniaxial extension data of 14 (PGA, 91k, $\chi_c = 46\%$); PMMG4 (4% Me, 81k, $\chi_c = 39\%$) and PMMG9 (9% Me, 46k, $\chi_c = 25\%$); and PGL2 (8% Me, 73k, $\chi_c = 27\%$) and PGL3 (4% Me, 102k, $\chi_c = 45\%$), extended at 5 mm·min⁻¹, with the break point indicated by X.

ultimate tensile strength even though it possessed a lower degree of crystallinity. Furthermore, PMMG with 9% methyl incorporation showed higher toughness than PGL. These experiments suggested that distinct methyl distribution in the polymer backbone resulted in discernable changes in mechanical properties.

Barrier Properties of PGA Homopolymer, and PGL and PMMG Copolymers. Thin films of PGA-based polymer samples were cast from HFIP solution for barrier testing. Prior to casting the films, polymer samples were dried in a vacuum oven for at least 4 days to remove any moisture and dissolved in HFIP completely at 60 °C at the initial polymer concentrations of 4–6 wt %. Polymer sheets were cast using a casting blade onto fluorinated ethylene propylene (FEP) thin-film surface. Then, they were air-dried at room temperature for 16 h and vacuum-dried at room temperature for 24 h. The resulting thin-film samples with an average thickness of 25 μm were opaque due to the high levels of crystallinity (30–42%) (Figure 7A–E).

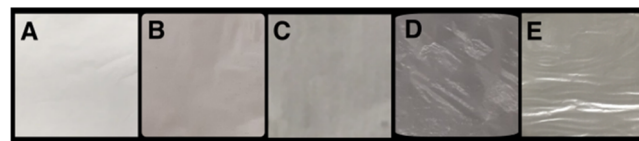


Figure 7. Tape-casted PGA film samples: (A) 14 (PGA, 0% Me); (B) PMMG4 (4% Me); (C) PGL3 (4% Me); (D) PMMG10 (8% Me); and (E) PGL2 (8% Me).

Oxygen permeation (OP) and water vapor permeation (WP) were measured for nonoriented solvent-cast films of PGA, PGL, and PMMG samples (Figure 8 and Table S4). OP at 23 °C and 0% relative humidity (RH) of PGA film was 4.6 cc·mil·m⁻²·d⁻¹·atm⁻¹, which was higher than that of biaxially oriented PGA (Kuredux, 0.6 cc·mil·m⁻²·d⁻¹·atm⁻¹) reported by Kureha according to ISO-15105-2 at 50% RH.⁵¹ Presumably, lower OP of Kuredux is likely a result of biaxially oriented films. Stretching films in one direction (uniaxially oriented) or two directions (biaxially oriented) reduces

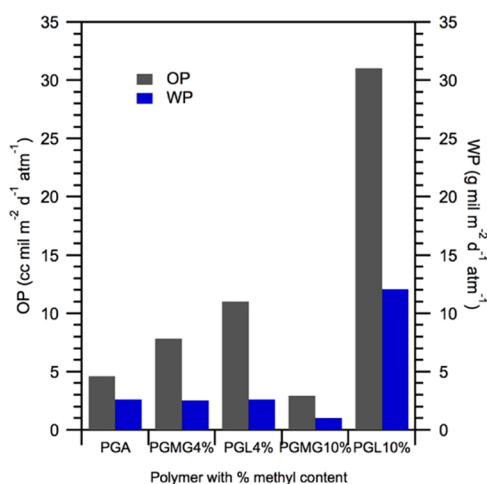


Figure 8. (A) Oxygen and (B) water vapor permeability of PGA-based polymers as a function of methyl content. PGA (11, 86k, $\chi_c = 45\%$), PGMG_{4%} (PGMG4, 81k, $\chi_c = 35\%$), PGL_{4%} (PGL3, 102k, $\chi_c = 31\%$), PGMG_{10%} (PGMG6, 27k, $\chi_c = 31\%$), PGL_{10%} (PGL4, 86k, $\chi_c = 30\%$).

molecular orientation and polymer fractional free volume and thus enhances crystallinity. In general, biaxially oriented films have lower permeability compared to nonoriented films due to strain-induced crystallization. However, WP (90% RH and 38 °C) of PGA homopolymer film (11, 2.6 g·mil·m⁻²·d⁻¹) was lower than that of PGA reported by Kureha (7.9 g·mil·m⁻²·d⁻¹).

O₂ permeation and water vapor permeation studies were conducted for PGL_{4%}, PGL_{10%}, PGMG_{4%}, and PGMG_{10%} copolymer samples using the same conditions. At low lactide loading (4% Me), O₂ permeation for PGL_{4%} was found to be 11 cc·mil·m⁻²·d⁻¹·atm⁻¹, which significantly increased to 32 cc·mil·m⁻²·d⁻¹·atm⁻¹ when methyl content was increased to 10%. At a low methyl loading (4%) using L, WP was found similar to pure PGA sample (2.6 g·mil·m⁻²·d⁻¹·atm⁻¹); however, a significant increase in water vapor permeation (12 g·mil·m⁻²·d⁻¹·atm⁻¹) was observed when % Me was increased to 10%. In comparison to PGL copolymers, O₂ and water vapor permeation values were preserved when 4% Me was incorporated using MG (OP = 7.8 cc·mil·m⁻²·d⁻¹·atm⁻¹ and WP = 2.5 g·mil·m⁻²·d⁻¹·atm⁻¹). More impressively, when the % Me was increased to 10% using MG, OP and WP both decreased by about 50% to 2.9 cc·mil·m⁻²·d⁻¹·atm⁻¹ and to 1.0 g·mil·m⁻²·d⁻¹·atm⁻¹, respectively, compared to PGA homopolymer. However, further increasing the methyl group content to 25% (PGMG_{25%}) results in an amorphous polymer (Table S2).

A combination of factors, such as spherulite size, morphology, and polymer crystallinity, has an effect on the barrier performance. PGMG samples showed comparable gas permeability to PGA and lower gas permeability than PGL even with the similar levels of % methyl groups in the backbone. Presumably, this was because methyl glycolide and glycolide units co-crystallized in PGMG. In addition, an increase in hydrophobicity with insertion of methyl group likely contributes to having superior performance in terms of water vapor permeation. The gas permeability of PGMG samples was not well correlated to the degree of crystallinity. Therefore, barrier properties of PGMG samples seem to be controlled by other factors, such as size of the crystallites/

nucleation density in addition to the degree of crystallinity.⁵² On the contrary, PGL samples have higher gas permeability than PGA because of lower degrees of crystallinity, suggesting that two methyl groups between PGA units substantially altered and deteriorated the barrier performance of PGA. In conclusion, these different results between PGL and PGMG indicated that distribution of methyl groups in the PGA backbone was important for gas permeability.

CONCLUSIONS

Bismuth (III) subsalicylate was found to be the most effective catalyst to prepare high-molar-mass PGA samples with $M_{n,SEC}$ up to 108 kg·mol⁻¹ within 10 min through ring-opening transesterification polymerization. Using the same approach, a series of well-defined PGL and PGMG copolymers with high-molar-masses and low methyl composition (4–10%) were synthesized. Different methyl distributions were imparted in the polymer backbone based on the comonomer used and resulted in a change in copolymer microstructure, crystallization behavior, and thermal, mechanical, and barrier properties. As we increased the methyl group content in the copolymers, the degradation temperature of the copolymers did not significantly change, but the melting temperature decreased. This resulted in an increase of $T_{d,5\%} - T_m$ from 76 to 89 °C, therefore widening the processing window. A substantial decrease in T_m from 222 to 182 °C and in χ_c from 45 to 11% was observed with 9% Me inclusion. Interestingly, PGL8% and PGMG9% have different melting temperatures, enthalpies of melting, and crystallization behaviors. Results from the mechanical tests suggested that the resulting polymers were brittle due to the crystallinity with ultimate tensile strengths up to 12 MPa and 8% strain at break. Nonoriented solvent-cast PGA films provided a slightly higher oxygen (4.6 cc·mil·m⁻²·d⁻¹·atm⁻¹) and water vapor (2.6 g·mil·m⁻²·d⁻¹·atm⁻¹) permeations comparable to commercial PGA materials. Incorporation of methyl group using lactide significantly increased OP and WP, especially at 10% Me insertion (OP = 32 cc·mil·m⁻²·d⁻¹·atm⁻¹ and WP = 12 g·mil·m⁻²·d⁻¹·atm⁻¹). In contrast, the copolymer materials manufactured using MG possessed improved barrier properties (2.9 cc·mil·m⁻²·d⁻¹·atm⁻¹ of OP and 1.0 g·mil·m⁻²·d⁻¹·atm⁻¹ of WP) compared to those using L. These data suggested that the distribution of methyl groups along the backbone was important for the thermal, mechanical, and gas barrier properties in these sustainable materials. To better understand these behaviors, more studies on the effect of morphological parameters on mechanical and gas barrier properties could be an interesting direction for further research.

ASSOCIATED CONTENT

Supporting Information

The Supporting Information is available free of charge at <https://pubs.acs.org/doi/10.1021/acs.biomac.1c00269>.

1D and 2D nuclear magnetic resonance spectra, size exclusion chromatography data, thermogravimetric analysis data, mechanical properties data, and oxygen permeability and water vapor permeability data (PDF)

Accession Codes Primary data files (NMR spectroscopy, DSC, TGA, SEC, WAXD, and tensile testing data) are available free of charge at <https://doi.org/10.13020/y5cb-bg84>

■ AUTHOR INFORMATION

Corresponding Author

Marc A. Hillmyer – Department of Chemistry, University of Minnesota, Minneapolis, Minnesota 55455-0431, United States; orcid.org/0000-0001-8255-3853; Email: hillmyer@umn.edu

Authors

Esra Altay – Department of Chemistry, University of Minnesota, Minneapolis, Minnesota 55455-0431, United States

Yoon-Jung Jang – Department of Chemistry, University of Minnesota, Minneapolis, Minnesota 55455-0431, United States

Xiang Qi Kua – Department of Chemistry, University of Minnesota, Minneapolis, Minnesota 55455-0431, United States

Complete contact information is available at:
<https://pubs.acs.org/10.1021/acs.biomac.1c00269>

Author Contributions

[†]E.A. and Y.-J.J. contributed equally to this work.

Notes

The authors declare no competing financial interest.

■ ACKNOWLEDGMENTS

The authors thank Braskem for financial support of this work. They also thank the National Science Foundation Center for Sustainable Polymers at the University of Minnesota, which is a National Science Foundation-supported Center for Chemical Innovation (CHE-1901635). The authors thank Dr. Jason Clark at Braskem for helpful discussions. They thank Dr. Christopher DeRosa at the University of Minnesota for helpful discussions. They thank Donald Massey at Clemson University for assistance with gas barrier measurements. WAXD data were obtained in the Characterization Facility, University of Minnesota, which receives partial support from NSF through MRSEC program.

■ REFERENCES

- (1) Dechy-Cabaret, O.; Martin-Vaca, B.; Bourissou, D. Controlled Ring-Opening Polymerization of Lactide and Glycolide. *Chem. Rev.* **2004**, *104*, 6147–6176.
- (2) Platel, R. H.; Hodgson, L. M.; Williams, C. K. Biocompatible Initiators for Lactide Polymerization. *Polym. Rev.* **2008**, *48*, 11–63.
- (3) Williams, C. K.; Hillmyer, M. A. Polymers from Renewable Resources: A Perspective for a Special Issue of Polymer Reviews. *Polym. Rev.* **2008**, *48*, 1–10.
- (4) Yang, Z.-Y.; Chen, C.-W.; Rwei, S.-P. Influence of Asymmetric Substituent Group 2-Methyl-1,3-Propanediol on Bio-Based Poly-(Propylene Furandicarboxylate) Copolyesters. *Soft Matter* **2020**, *16*, 402–410.
- (5) Frazza, E. J.; Schmitt, E. E. A New Absorbable Suture. *J. Biomed. Mater. Res.* **1971**, *5*, 43–58.
- (6) Kuredux Polyglycolic Acid (PGA) Technical Guidebook. http://www.Kureha.Com/Pdfs/Kuredux_technical.Pdf (accessed September 6, 2020).
- (7) Samantaray, P. K.; Little, A.; Haddleton, D. M.; McNally, T.; Tan, B.; Sun, Z.; Huang, W.; Ji, Y.; Wan, C. Poly(Glycolic Acid) (PGA): A Versatile Building Block Expanding High Performance and Sustainable Bioplastic Applications. *Green Chem.* **2020**, *22*, 4055–4081.
- (8) Miltenberger, K. *Ullmann's Encyclopedia of Industrial Chemistry*; Wiley-VCH Verlag GmbH & Co. KGaA, 2000.
- (9) Iglesias, J.; Martínez-Salazar, I.; Maireles-Torres, P.; Martín Alonso, D.; Mariscal, R.; López Granados, M. Advances in Catalytic Routes for the Production of Carboxylic Acids from Biomass: A Step Forward for Sustainable Polymers. *Chem. Soc. Rev.* **2020**, *49*, 5704–5771.
- (10) Yamane, K.; Sato, H.; Ichikawa, Y.; Sunagawa, K.; Shigaki, Y. Development of an Industrial Production Technology for High-Molecular-Weight Polyglycolic Acid. *Polym. J.* **2014**, *46*, 769–775.
- (11) Schwarz, K.; Epple, M. A Detailed Characterization of Polyglycolide Prepared by Solid-State Polycondensation Reaction. *Macromol. Chem. Phys.* **1999**, *200*, 2221–2229.
- (12) Epple, M.; Herzberg, O. Polyglycolide with Controlled Porosity: An Improved Biomaterial. *J. Mater. Chem.* **1997**, *7*, 1037–1042.
- (13) Pinkus, A. G.; Subramanyam, R. New High-Yield, One-Step Synthesis of Polyglycolide from Haloacetic Acids. *J. Polym. Sci., Polym. Chem. Ed.* **1984**, *22*, 1131–1140.
- (14) Ayyoob, M.; Lee, D. H.; Kim, J. H.; Nam, S. W.; Kim, Y. J. Synthesis of Poly(Glycolic Acids) via Solution Polycondensation and Investigation of Their Thermal Degradation Behaviors. *Fibers Polym.* **2017**, *18*, 407–415.
- (15) Takahashi, K.; Taniguchi, I.; Miyamoto, M.; Kimura, Y. Melt/Solid Polycondensation of Glycolic Acid to Obtain High-Molecular-Weight Poly(Glycolic Acid). *Polymer* **2000**, *41*, 8725–8728.
- (16) Göktürk, E.; Pemba, A. G.; Miller, S. A. Polyglycolic Acid from the Direct Polymerization of Renewable C1 Feedstocks. *Polym. Chem.* **2015**, *6*, 3918–3925.
- (17) Lu, Y.; Swisher, J. H.; Meyer, T. Y.; Coates, G. W. Chirality-Directed Regioselectivity: An Approach for the Synthesis of Alternating Poly(Lactic-Co-Glycolic Acid). *J. Am. Chem. Soc.* **2021**, *143*, 4119–4124.
- (18) Gilding, D. K.; Reed, A. M. Biodegradable Polymers for Use in Surgery—Polyglycolic/Poly(Actic Acid) Homo- and Copolymers: 1. *Polymer* **1979**, *20*, 1459–1464.
- (19) Dong, C.-M.; Qiu, K.-Y.; Gu, Z.-W.; Feng, X.-D. Synthesis of Poly(D,L-Lactic Acid-Alt-Glycolic Acid) from D,L-3-Methylglycolide. *J. Polym. Sci., Part A: Polym. Chem.* **2000**, *38*, 4179–4184.
- (20) Kaihara, S.; Matsumura, S.; Mikos, A. G.; Fisher, J. P. Synthesis of Poly(L-Lactide) and Polyglycolide by Ring-Opening Polymerization. *Nat. Protoc.* **2007**, *2*, 2767–2771.
- (21) Gautier, E.; Fuertes, P.; Cassagnau, P.; Pascault, J.-P.; Fleury, E. Synthesis and Rheology of Biodegradable Poly(Glycolic Acid) Prepared by Melt Ring-Opening Polymerization of Glycolide. *J. Polym. Sci., Part A: Polym. Chem.* **2009**, *47*, 1440–1449.
- (22) Duval, C.; Nouvel, C.; Six, J.-L. Is Bismuth Subsalicylate an Effective Nontoxic Catalyst for Plga Synthesis? *J. Polym. Sci., Part A: Polym. Chem.* **2014**, *52*, 1130–1138.
- (23) Pascual, A.; Leiza, J. R.; Mecerreyes, D. Acid Catalyzed Polymerization of Macrolactones in Bulk and Aqueous Miniemulsion: Ring Opening vs. Condensation. *Eur. Polym. J.* **2013**, *49*, 1601–1609.
- (24) Zhou, X.; Hong, L. Controlled Ring-Opening Polymerization of Cyclic Esters with Phosphoric Acid as Catalysts. *Colloid Polym. Sci.* **2013**, *291*, 2155–2162.
- (25) Makiguchi, K.; Kikuchi, S.; Yanai, K.; Ogasawara, Y.; Sato, S.; Satoh, T.; Kakuchi, T. Diphenyl Phosphate/4-Dimethylaminopyridine as an Efficient Binary Organocatalyst System for Controlled/Living Ring-Opening Polymerization of L-Lactide Leading to Diblock and End-Functionalized Poly(L-Lactide)S. *J. Polym. Sci., Part A: Polym. Chem.* **2014**, *52*, 1047–1054.
- (26) Makiguchi, K.; Satoh, T.; Kakuchi, T. Diphenyl Phosphate as an Efficient Cationic Organocatalyst for Controlled/Living Ring-Opening Polymerization of δ -Valerolactone and ϵ -Caprolactone. *Macromolecules* **2011**, *44*, 1999–2005.
- (27) Dove, A. P. Organic Catalysis for Ring-Opening Polymerization. *ACS Macro Lett.* **2012**, *1*, 1409–1412.
- (28) Kricheldorf, H. R. Syntheses of Biodegradable and Biocompatible Polymers by Means of Bismuth Catalysts. *Chem. Rev.* **2009**, *109*, 5579–5594.

- (29) Kricheldorf, H. R.; Rost, S. Copolymerizations of ϵ -Caprolactone and Glycolide A Comparison of Tin(II)Octanoate and Bismuth(III)Subsalicylate as Initiators. *Biomacromolecules* **2005**, *6*, 1345–1352.
- (30) Kricheldorf, H. R.; Behnken, G. Copolymerizations of Glycolide and L-Lactide Initiated with Bismuth(III)N-Hexanoate or Bismuth Subsalicylate. *J. Macromol. Sci., Part A* **2007**, *44*, 795–800.
- (31) Lu, Y.; Schmidt, C.; Beuermann, S. Fast Synthesis of High-Molecular-Weight Polyglycolide Using Diphenyl Bismuth Bromide as Catalyst. *Macromol. Chem. Phys.* **2015**, *216*, 395–399.
- (32) Gao, J.; Yuan, Y.; Cui, A.-J.; Tian, F.; Chen, S.-C.; He, M.-Y.; Chen, Q. Bismuth(III) Complexes Based on Bis(Triazol) Ligands: Effect of Fluorine Substitution on the Structure and Catalysis for the Polymerization of Glycolide. *Z. Anorg. Allg. Chem.* **2016**, *642*, 698–703.
- (33) Balasanthiran, V.; Beilke, T. L.; Chisholm, M. H. Use of over the Counter Oral Relief Aids or Dietary Supplements for the Ring-Opening Polymerization of Lactide. *Dalton Trans.* **2013**, *42*, 9274–9278.
- (34) Cooper, D. R.; Sutton, G. J.; Tighe, B. J. Poly α -Ester Degradation Studies. V. Thermal Degradation of Polyglycolide. *J. Polym. Sci., Polym. Chem. Ed.* **1973**, *11*, 2045–2056.
- (35) Yamane, K.; Miura, H.; Ono, T.; Nakajima, J.; Itoh, D. Crystalline Polyglycolic Acid, Polyglycolic Acid Composition and Production Process Thereof. European Patent EP1 914 258 B12008.
- (36) Murcia Valderrama, M. A.; van Putten, R.-J.; Gruter, G.-J. M. PLGA Barrier Materials from CO₂. The Influence of Lactide Co-Monomer on Glycolic Acid Polyesters. *ACS Appl. Polym. Mater.* **2020**, *2*, 2706–2718.
- (37) Hosoya, K.; Maruyama, T.; Fujiki, T.; Tanaka, N.; Araki, M. A Convenient Synthetic Method of Unsymmetrically Substituted Chiral Lactone Using Liquid-Solid Biphasic System. *Chem. Express* **1990**, *21*, 149–152.
- (38) Dong, C.-M.; Qiu, K.-Y.; Gu, Z.-W.; Feng, X.-D. Living Polymerization of D,L-3-Methylglycolide Initiated with Bimetallic (Al/Zn) μ -Oxo Alkoxide and Copolymers Thereof. *J. Polym. Sci., Part A: Polym. Chem.* **2001**, *39*, 357–367.
- (39) Dong, C.-M.; Qiu, K.-Y.; Gu, Z.-W.; Feng, X.-D. Synthesis of Star-Shaped Poly(d,l-Lactic Acid-Alt-Glycolic Acid) with Multifunctional Initiator and SnOct₂ Catalyst. *Polymer* **2001**, *42*, 6891–6896.
- (40) Zhang, X.; He, Q.; Chen, Q.; Nealey, P. F.; Ji, S. Directed Self-Assembly of High χ Poly(Styrene-*b*-(Lactic Acid-Alt-Glycolic Acid)) Block Copolymers on Chemical Patterns via Thermal Annealing. *ACS Macro Lett.* **2018**, *7*, 751–756.
- (41) Schneiderman, D. K.; Hillmyer, M. A. Aliphatic Polyester Block Polymer Design. *Macromolecules* **2016**, *49*, 2419–2428.
- (42) Liu, J.; Zhang, C.; Li, Z.; Zhang, L.; Xu, J.; Wang, H.; Xu, S.; Guo, T.; Yang, K.; Guo, K. Dibutyl Phosphate Catalyzed Commercial Relevant Ring-Opening Polymerizations to Bio-Based Polyesters. *Eur. Polym. J.* **2019**, *113*, 197–207.
- (43) Kricheldorf, H. R.; Kreiser-Saunders, I.; Stricker, A. Polylactones 48. SnOct₂-Initiated Polymerizations of Lactide: A Mechanistic Study. *Macromolecules* **2000**, *33*, 702–709.
- (44) Witzke, D. R.; Narayan, R.; Kolstad, J. J. Reversible Kinetics and Thermodynamics of the Homopolymerization of L-Lactide with 2-Ethylhexanoic Acid Tin(II) Salt. *Macromolecules* **1997**, *30*, 7075–7085.
- (45) Takojima, K.; Makino, H.; Saito, T.; Yamamoto, T.; Tajima, K.; Isono, T.; Satoh, T. An Organocatalytic Ring-Opening Polymerization Approach to Highly Alternating Copolymers of Lactic Acid and Glycolic Acid. *Polym. Chem.* **2020**, *11*, 6365–6373.
- (46) Yamane, K.; Sato, H.; Kawakami, Y. Polyglycolic Acid-Based Resin Composition and Shaped Product Thereof. U.S. Patent US7,179,868 B22007.
- (47) Yu, C.; Bao, J.; Xie, Q.; Shan, G.; Bao, Y.; Pan, P. Crystallization Behavior and Crystalline Structural Changes of Poly(Glycolic Acid) Investigated via Temperature-Variable WAXD and FTIR Analysis. *CrystEngComm* **2016**, *18*, 7894–7902.
- (48) Abe, S. Sequentially Biaxially-Oriented Polyglycolic Acid Film, Production Process Thereof and Multi-Layer Film. U.S. Patent US2011/0027590 A12011.
- (49) Tsuji, H.; Kikkawa, K.; Arakawa, Y. Cocrystallization of Monomer Units of Biobased and Biodegradable Poly(L-Lactic Acid-Co-Glycolic Acid) Random Copolymers. *Polym. J.* **2018**, *50*, 1079–1088.
- (50) Kuredux Mechanical Properties. <http://www.kuredux.com/en/about/properties.html> (accessed April 05, 2021).
- (51) Ito, D.; Takatsuji, K. In *Barrier Properties and Characteristics of Polyglycolic Acid for Un-Oriented and Oriented Films*, Annual Technical Conference—ANTEC, 2011; pp 2608–2614.
- (52) Drieskens, M.; Peeters, R.; Mullens, J.; Franco, D.; Lemstra, P. J.; Hristova-Bogaerds, D. G. Structure versus Properties Relationship of Poly(Lactic Acid). I. Effect of Crystallinity on Barrier Properties. *J. Polym. Sci., Part B: Polym. Phys.* **2009**, *47*, 2247–2258.